Available online at www.sciencedirect.com
SCIENCE DIRECT®

Journal of the European Ceramic Society 23 (2003) 1383–1390
www.elsevier.com/locate/jeurceramsoc

The influence of concentration on the formation of $BaTiO_3$ by direct reaction of $TiCl_4$ with $Ba(OH)_2$ in aqueous solution

M. Viviani[a], M.T. Buscaglia[a], A. Testino[b], V. Buscaglia[a,*], P. Bowen[c], P. Nanni[b]

[a]*Institute for Energetics and Interphases (IENI-CNR), National Research Council, via De Marini 6, I-16149 Genoa, Italy*
[b]*Department of Process and Chemical Engineering, University of Genoa, Fiera del Mare, Pad. D, I-16129 Genoa, Italy*
[c]*Department of Materials Science, Powder Technology Laboratory, Swiss Federale Institute of Technology (EPFL), CH-1015 Lausanne, Switzerland*

Received 15 March 2002; received in revised form 6 September 2002; accepted 16 September 2002

Abstract

The formation of fine $BaTiO_3$ particles by reaction between liquid $TiCl_4$ and $Ba(OH)_2$ in aqueous solution at 85 °C and pH $\geqslant$ 13 has been studied for $0.062 \leqslant [Ba^{2+}] \leqslant 0.51$ mol l^{-1}. The concentration of Ba^{2+} ions has a strong influence on reaction kinetics, particle size and crystallite size. When $[Ba^{2+}] > \approx 0.12$ mol l^{-1}, the precipitate consists of nanosized (≈30 nm) to submicron (100–300 nm) particles of crystalline $BaTiO_3$. At lower concentrations, the final product is a mixture of crystalline $BaTiO_3$ and a Ti-rich amorphous phase even for very long reaction times. A two-steps precipitation mechanism is proposed. Initially, a Ti-rich amorphous precipitate is rapidly produced. Reaction between the amorphous phase and the Ba^{2+} ions left in solution then leads to crystallisation of $BaTiO_3$. In addition to nucleation and growth of nanocrystals, the final size and morphology of $BaTiO_3$ particles obtained at low concentration can be determined by aggregation of nanocrystals and heterogeneous nucleation on existing crystal surfaces.

Keywords: $BaTiO_3$; Particles; Perovskites; Powders: chemical preparation, Titanates

1. Introduction

Barium titanate, $BaTiO_3$, is a ferroelectric ceramic material extensively used as dielectric in ceramic capacitors and, in particular, in multilayer ceramic capacitors (MLCCs) because of its high permittivity and low losses.[1] Other applications include embedded capacitance in printed circuit boards (PCB), PTCR thermistors and piezoelectric devices like underwater transducers. Recent advances in microelectronics and communications have led to the miniaturisation of MLCCs. Higher capacitance in smaller case sizes requires a reduction of the thickness of the ceramic layers below 2–3 μm and the increase of the number of layers (>200). To achieve this goal, powders with improved quality, small and uniform size (of the order of 100 nm) are required. Conventional $BaTiO_3$ powders obtained by solid-state reaction between TiO_2 and $BaCO_3$ or by the oxalate route are generally rather coarse, poorly uniform and, therefore, not always suitable to realise very thin layers. As can be seen from available reviews,[2,3] many chemical methods were proposed for the synthesis of high quality $BaTiO_3$ powders. Among them, the hydrothermal and sol-gel methods are the most promising from the point of view of stoichiometry control, reproducibility, purity and particle size. The hydrothermal route has the additional advantage to lead directly to crystalline powders at rather low temperatures.[4–12] The hydrothermal process is carried out by suspending TiO_2 particles or a TiO_2 gel in an aqueous $Ba(OH)_2$ solution and then autoclaving at 150–300 °C. The general thermodynamic analysis of hydrothermal synthesis of $BaTiO_3$ and other perovskites in aqueous medium was presented by Lencka and Riman.[13,14] According to their results, the stable solid phase in a wide pH-$[Ba^{2+}]$ field is $BaTiO_3$ and quantitative precipitation of the perovskite is possible even at temperatures below 100 °C. The presence of CO_2 must be avoided, otherwise the product will be always contaminated by $BaCO_3$.[13] In recent years an increasing

* Corresponding author. Tel.: +39-010-647-5708; fax: +39-010-647-5700.
E-mail address: buscaglia@icfam.ge.cnr.it (V. Buscaglia).

0955-2219/02/$ - see front matter © 2002 Elsevier Science Ltd. All rights reserved.
PII: S0955-2219(02)00357-6

interest has been focused on the direct precipitation of $BaTiO_3$ in aqueous medium using solutions of inorganic or organo-metallic compounds.[10,15–22] The size of the particles that precipitate out of solution depends, in general, on the relative rates of nuclei formation and crystallite growth. Both nucleation and growth are very sensitive to temperature, concentration and mixing conditions. A careful control of the above parameters should allow the production of particles with the desired size, from micron- to nano-scale. A further advantage is that the preliminary preparation of a suitable solid (either amorphous or crystalline) or gel precursor as a titanium source and the related manipulations are avoided. The realisation of a continuous production process is also greatly facilitated by the use of solutions.[18,22]

In this paper the experimental results about the influence of $[Ba^{2+}]$ and reaction time on the formation of $BaTiO_3$ by direct addition of liquid $TiCl_4$ to aqueous solutions of $Ba(OH)_2$ at 85 °C are presented and discussed. One of the goals of the present study is to show that the concentration of Ba^{2+} ions is a key parameter in the formation of $BaTiO_3$ because the precipitation of $BaTiO_3$, even if possible from the thermodynamic point of view over a wide concentration range, can be strongly affected by kinetic factors.

2. Experimental

Barium titanate was prepared by precipitation in aqueous solution according to the overall reaction

$$Ba(OH)_2(aq) + TiCl_4(l) + 4NaOH(aq) \rightarrow BaTiO_3(s) + 4NaCl(aq) + 3H_2O(l) \quad (1)$$

where (aq) denotes a species in solution. Commercial reactants ($Ba(OH)_2$*$8H_2O$, 98%, Sigma Aldrich; NaOH, 97%, Sigma Aldrich; $TiCl_4$, 99,9%, Acros) were employed. Precipitation was carried out at 85 °C in a closed PTFE vessel containing NaOH and $Ba(OH)_2$ dissolved in freshly distilled water. The temperature was controlled by means of a thermostatic bath. Different initial concentrations of $Ba(OH)_2$ where adopted: 0.062, 0.086, 0.114, 0.18, 0.31 and 0.51 mol/l. An excess of NaOH in comparison to the stoichiometric amount required by reaction (1) was used to maintain a $pH \geqslant 13$ during the entire course of reaction. The pH-$[Ba^{2+}]$ conditions adopted should guarantee, according to the thermodynamic calculations of Lencka and Riman,[13,14] a quantitative precipitation of $BaTiO_3$ (yield > 99.9%) at 85 °C. Titanium tetrachloride was directly injected inside the solution while stirring. The formation of a white precipitate was observed. In all experiments the vessel was filled with 1000 cm^3 of solution and the addition of $TiCl_4$ was performed at a flow rate of 3 cm^3 min^{-1}. The precipitate was then aged at 85 °C for different times from 15 min to 120 h under stirring. The resulting suspension was transferred in a second closed vessel by means of a peristaltic pump and washed with freshly distilled water until chloride ions were no longer present in the supernatant. Finally the powder was oven dried at 80 °C. All the synthesis steps ($TiCl_4$ addition, precipitate ageing, transfer to the washing vessel, final washing) were performed under inert atmosphere by circulating a purified nitrogen stream inside the vessels to avoid contact with atmospheric CO_2. The as-prepared powders collected under different conditions of concentration and ageing time were characterised by different techniques. Particle morphology was observed by scanning electron microscopy (SEM, Philips 515) and transmission electron microscopy (TEM, Jeol J2010). The density of powders, ρ, was measured by means of helium pycnometry (Micromeritics AccuPyc 1330). Specific surface area, S_{BET}, measurements were performed by isothermal nitrogen physisorption (BET method, Micromeritics ASAP 2010). The equivalent BET particle diameter, d_{BET}, was calculated by the formula $d_{BET} = 6/\rho S_{BET}$. Thermogravimetry and thermal differential analysis (TG/DTA, Setaram 92-16.18) was performed up to 1300 °C in dry air. Lattice parameters of $BaTiO_3$ were determined by X-ray diffraction (XRD, Philips PW1710, CoK_α radiation). The crystallite size of $BaTiO_3$, d_{XRD}, was obtained from the broadening of the (111) diffraction peak by means of Scherrer equation[23] after correction for instrumental broadening. A negligible contribution of the microscopic strain to broadening was assumed. The resulting size can be interpreted as an average crystal dimension perpendicular to the (111) crystallographic planes. To detect the presence of any amorphous phase with composition different from that of $BaTiO_3$, even present in a small amount not directly detectable by XRD on the as-prepared product, the powders were calcined at 950 °C for 4 h. Phase composition after annealing is very sensitive to the overall Ba/Ti molar ratio of the solid. According to the $BaO–TiO_2$ phase diagram[24,25] the calcined (950 °C) samples should be a mixture of $BaTiO_3$ and $BaTi_2O_5$ for $0.5 < Ba/Ti < 1$, a mixture of $BaTi_2O_5$ and $Ba_4Ti_{13}O_{30}$ for $0.31 < Ba/Ti < 0.5$, etc. Quantitative phase composition was thus obtained by the Rietveld method (Cerius^2 software, Molecular Simulations Inc.) and the corresponding Ba/Ti molar ratio was calculated. The reliability of this procedure was established by measuring the Ba/Ti ratio on the samples prepared from $[Ba^{2+}] = 0.086$ mol/l using atomic adsorption spectroscopy (Perkin Elmer AAnalyst-100). The agreement of the two series of measurements was within ±2%. For nearly stoichiometric powders, the Ba/Ti ratio was also

measured by inductively coupled plasma spectroscopy (ICP, Perkin Elmer Plasma 2000). The amount of crystalline phase in powders obtained from the 0.062M solution was measured by quantitative XRD. For this purpose the internal standard method described by Klug and Alexander[26] was adopted. A calibration curve was established using synthetic mixtures of fine $BaTiO_3$ (from 5 to 50 wt.%) and the amorphous phase. The amorphous phase was that corresponding to the precipitate obtained from the 0.062 M solution after 1.5 h ageing, where the crystalline phase was below the XRD detection limit. Silicon was added to each sample as internal standard in the constant proportion of 40 wt.%. The ratio of the integrated intensity of the (111) reflection of $BaTiO_3$ to the integrated intensity of the (100) reflection of silicon was plotted against the weight fraction of $BaTiO_3$. Each point was the average of five determinations. The resulting calibration curve was closely approximated by a straight line. The procedure described above relies on the hypothesis of constant composition of the amorphous phase with time.

3. Results

3.1. Ba/Ti ratio

The variation of the Ba/Ti atomic ratio, R, of the precipitate collected at different times as a function of the initial barium concentration, $[Ba^{2+}]_0$, is shown in Fig. 1. For concentrations $\geqslant 0.18$ mol l^{-1}, stoichiometric and fully crystalline $BaTiO_3$ powders were obtained in a time $\leqslant 5$ h. When $[Ba^{2+}]_0 = 0.114$ mol l^{-1}, complete conversion of the precipitate in crystalline $BaTiO_3$ was attained only for times of the order of 100 h. At lower concentration, the precipitate consisted of a mixture of a Ti-rich amorphous phase and crystalline $BaTiO_3$. However, when $[Ba^{2+}]_0 = 0.062$ M, the amount of $BaTiO_3$ in the precipitate was below the XRD detection limit ($\approx$0.5 wt.%) for times up to 10 h and R took an almost constant value of $\approx$0.42 (see Fig. 1). The amorphous phase was a white powder with density of $\approx$4.7 g cm^{-3} after drying at 80 °C. When the predominant phase was $BaTiO_3$, the residual amorphous phase was hardly detectable by XRD. On the contrary, when a precipitate containing some amorphous phase ($R < 1$) was fired at 950 °C in a platinum crucible, the peaks of the $BaTi_2O_5$ phase appeared on the diffraction pattern. A Ti excess $\geqslant 2$ at.% ($R \leqslant 0.98$) can be detected by a careful collection of the diffraction profile. Traces of $BaCO_3$ ($\approx$1 wt.%) were detected in most of the as-prepared powders, but they disappeared after thermal treatment. The Ba/Ti atomic ratio of the powders completely transformed in $BaTiO_3$ ($[Ba^{2+}]_0 \geqslant 0.18$M) accordingly to XRD were almost stoichiometric at ICP spectroscopy: $R = 1.01 \pm 0.02$. The amount of Na contained in the powders is generally < 800 ppm (ICP).

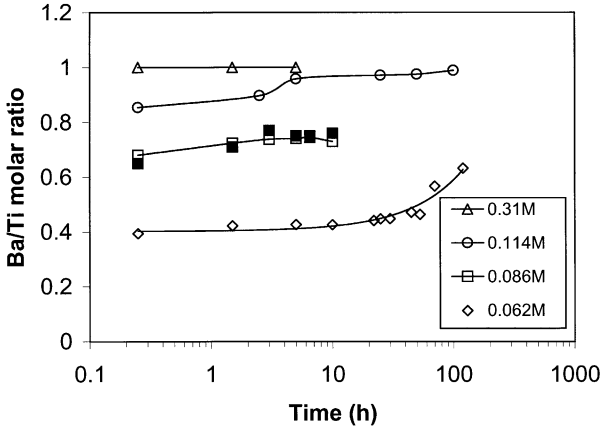

Fig. 1. Ba/Ti molar ratio of powders obtained at 85 °C for different values of the initial $Ba(OH)_2$ concentration. Open symbols: values obtained from Rietveld analysis of XRD patterns collected after 4 h annealing at 950 °C. Full symbols: values obtained from atomic adsorption spectroscopy. The lines were drawn only as a guide for eyes.

3.2. Crystal structure and crystallite size

The crystal structure of $BaTiO_3$ particles was pseudocubic in any case although the local structure is non centrosymmetric, as found by IR/Raman spectroscopy in a previous investigation.[27] The tetragonality of the structure, defined as the ratio c/a of the unit cell edges, is thus well below (probably < 1.003) that of single crystal $BaTiO_3$ (1.010) and then not detectable by ordinary XRD, also because of the broadening effect of the XRD peaks related to the small crystallite size. The pseudocubic unit cell edge, a, was then assumed as the representative crystallographic parameter. Normal crystallographic properties of $BaTiO_3$ are restored after annealing of powders at temperatures > 1000 °C. In general, the breadth of the diffraction peaks at half maximum after correction for instrumental broadening is dependent on both crystallite size and microstrain in the lattice. The two effects can be separated by means of the Williamson-Hall method.[28] Application to the present case has shown that the microstrain contribution to peak broadening is negligible for powders obtained from concentrated solutions, $[Ba^{2+}]_0 \geqslant 0.18$ mol l^{-1} and rather small ($\Delta d/d \leqslant 2 \times 10^{-3}$) for powders obtained at lower concentration. Consequently the Scherrer method can be considered sufficiently accurate for crystallite size determination. In addition, such a method can be applied even to samples containing a small amount of crystalline phase (0.062 M series, ageing time < 70 h) by careful overnight collection of the (111) peak. The XRD crystallite size is shown in Table 1. An estimate of the accuracy of the XRD measurements can be obtained by comparing d_{XRD} with d_{BET}. However, the comparison is

Table 1
Crystallite size, equivalent BET diameter and particle size for powders obtained from $Ba(OH)_2$ solutions at different concentration (ageing time at 85 °C is shown in parentheses)

$[Ba^{2+}]_0$ (mol l^{-1})	Crystallite size[a] (nm)	BET diameter[b] (nm)	Particle size[c] (nm)
0.062	from 29 (20 h) to 148 (120 h)		from ≈10 (0.25 h) to ≈10^3 (120 h)
0.086	93±9 (0.25–10 h)		50–300 (10 h)
0.114	57±9 (0.25–100 h)	66 (100 h)	70–170 (0.25 h) 70–300 (100 h)
0.18	60 (5 h)	65 (5 h)	50–250 (5 h)
0.31	38±2 (0.25–5 h)	32±2 (0.25–5 h)	20–60 (5 h)
0.51	20.9 (5 h)	24 (5 h)	20–50 (5 h)

[a] Scherrer equation.
[b] Reported only for single phase powders.
[c] From TEM and SEM observation.

meaningful only when no amorphous phase is present, i.e. for the powders obtained at high concentration (0.51–0.18 mol l^{-1}, 0.114 mol l^{-1} at long times). In such cases, the agreement (see Table 1) between the two series of measurements is within ±20%. When the precipitate contained a significant amount of the amorphous phase, S_{BET} rapidly increased and attained values of the order of 150 m^2/g when the amorphous phase was predominant. A significant growth of the crystallites with time at constant concentration was noticed only at the lowest value of $[Ba^{2+}]_0$, 0.062 mol l^{-1}. At higher concentration, the observed variations of d_{XRD} were within±20% the average value and therefore comparable with the error of technique. In general, the crystallite size increases as the concentration decreases. When the pseudocubic unit cell edge of $BaTiO_3$ is plotted against the crystallite size as shown in Fig. 2, a significant correlation is found and, in particular, a increases rapidly when the size decreases below ≈60 nm. The data corresponding to the 0.086 M solution show some deviation from this behaviour.

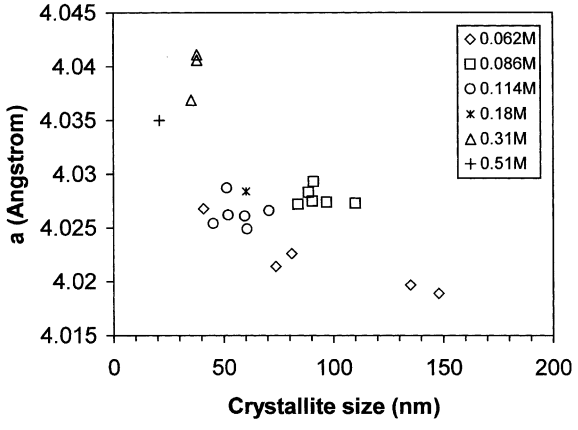

Fig. 2. Lattice parameter of the pseudocubic $BaTiO_3$ unit cell vs. crystallite size.

3.3. Particle morphology

The $BaTiO_3$ powders obtained at high concentration, 0.51 and 0.31 mol l^{-1}, were very fine and consisted of particles in the range 20–50 nm, according to SEM and TEM observation. Moreover, at TEM observation most particles corresponded to single nanocrystals. Accordingly, the size of the particles evaluated from SEM and TEM micrographs, was in good agreement with the XRD particle size as well as with the BET size (see Table 1). At intermediate concentrations, 0.18, 0.114 and 0.086 mol l^{-1}, the powders consisted of approximately spherical particles in the range ≈50 to ≈300 nm. The size of the smallest particles was comparable to d_{XRD} (60 nm for the 0.18 M/5 h sample and 57±9 nm for the 0.114 M samples, Table 1) and d_{BET} (65 nm for the 0.18 M/5 h sample and 66 nm for the 0.114 M/100 h sample, Table 1), whereas the larger particles were probably composed of tight aggregates of several crystallites. At the lowest concentration (0.062 mol^{-1}), SEM and TEM observation on powders with different ageing times, showed the progressive crystallisation of $BaTiO_3$ from the amorphous phase. At very short time (0.25 h) the precipitate contained only a limited number of very small $BaTiO_3$ crystals with a size of the order of 10 nm. In this condition the amorphous phase was mainly composed of spherical particles of 100–200 nm. At longer times, both the number of crystals and their size increased. The crystallisation of $BaTiO_3$ looks closely related to a progressive transformation of the amorphous spherical particles in aggregates of very small (<10 nm), but still amorphous particles. Small crystallites of $BaTiO_3$ were often observed inside these aggregates, but never associated with the larger spherical amorphous particles. The different morphologies, possibly corresponding to different stages of transformation, are shown in Fig. 3. SEM observation at lower magnification than that allowed by the TEM showed the growth of large, dendritic-like $BaTiO_3$ particles composed of crystals of 100–300 nm for times >50 h.

An example is given in Fig. 4. The observed morphological evolution is in qualitative agreement with the increase of crystallite size with ageing time detected by XRD.

3.4. Crystallization kinetics

The results of SEM and TEM observations strongly suggest that crystallization of $BaTiO_3$ at low concentration (0.062 M) is controlled by a nucleation and growth mechanism. Nucleation apparently occurs in the amorphous phase and the perovskite crystals grow at the expenses of the parent phase. The plot of the volume fraction of $BaTiO_3$ in the solid phase (see Fig. 5) shows a typical sigmoidal shape. As a first approximation, the crystallisation kinetics can be described by the Jonhson–Mehl–Avrami (JMA) equation[29]

$$\ln\ \ln\left(\frac{1}{1-\beta}\right) = \ln k + n\ln t \qquad (2)$$

where β is the volume fraction of $BaTiO_3$ in the precipitate, k is a kinetic constant and n is the time exponent. The result is shown in Fig. 5. The value of n resulting from linear regression is 2.3 ± 0.25 and that of k is 2.8×10^{-14} $s^{-2.3}$. The value of n depends on nature of the nucleation site as well as on the nucleation rate and on the growth-controlling mechanism (phase boundary reaction or diffusion).[29] The present value can be interpreted as the diffusion-controlled growth of particles of any shape from small dimensions and decreasing nucleation rate.

3.5. Thermogravimetry and density

DTA-TGA experiments were performed on powders completely transformed in $BaTiO_3$ ($[Ba^{2+}]_0 \geqslant 0.18$ M). All these powders showed a significant weight loss, ≈3.2 wt.% between 100 and 800 °C related to water

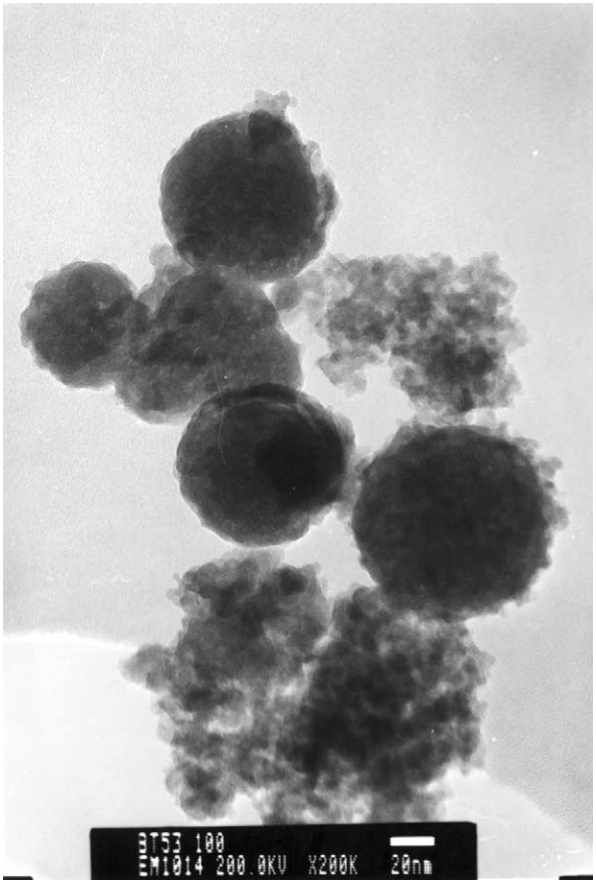

Fig. 3. Different morphologies observed (TEM) in a powder obtained from a 0.062 M solution of $Ba(OH)_2$ after 53 h ageing at 85 °C. The large spherical particles are amorphous, while the aggregates of small particles consist of both amorphous (Ti-rich) and crystalline ($BaTiO_3$) phases.

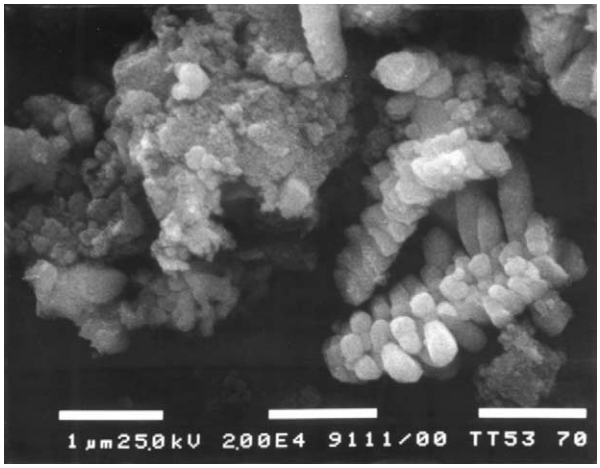

Fig. 4. SEM micrograph of a powder obtained from a 0.062 M solution of $Ba(OH)_2$ after 100 h ageing at 85 °C. Right side: dendritic-like particles of $BaTiO_3$. Left side: aggregate of amorphous and crystalline particles.

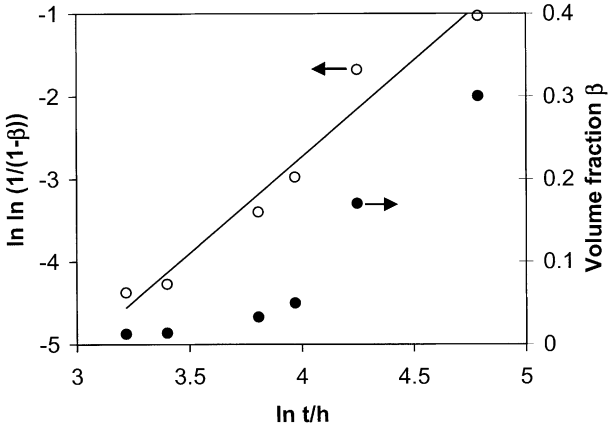

Fig. 5. Crystallisation kinetics (full symbols) and corresponding Avrami plot (open symbols) for the formation of $BaTiO_3$ from a 0.062 M solution of $Ba(OH)_2$ at 85 °C. The solid line represents the best fit to experimental values.

evaporation. Water release is significant when expressed on mol basis: ≈0.43 mol of H_2O per mol of $BaTiO_3$. Above 800 °C, an endothermic DTA peak associated with a small weight loss was observed. This contribution is usually associated to the release of CO_2 by reaction between traces of $BaCO_3$ and $BaTiO_3$ to form Ba_2TiO_4.[6,30] The density of the as-prepared powders was ≈5.25 g cm^{-3}, a value remarkably lower than the reference density of $BaTiO_3$, 6.02 g cm^{-3}. The rather high temperature at which water was released and the low density suggest the presence of OH^- lattice groups, a rather common circumstance in perovskite-like oxides.[31]

4. Discussion

On the basis of the above experimental results, the formation of $BaTiO_3$ by reaction between a $Ba(OH)_2$ aqueous solution (pH > 13) and liquid $TiCl_4$ at 85 °C [Reaction (1)] can be described by a two-steps process: (i) precipitation of a Ti-rich amorphous phase; (ii) crystallization of $BaTiO_3$ by reaction between the amorphous phase and the Ba^{2+} ions left in solution. Step 1 is in any case very fast, while the kinetics of step 2 is strongly dependent on barium concentration in the starting solution. Lowering $[Ba^{2+}]_0$ from 0.5 to 0.06 mol l^{-1}, the crystallisation rate decreases by several orders of magnitude. A critical concentration threshold of ≈0.12 mol l^{-1} can be defined. Above this value, complete conversion to $BaTiO_3$ can be attained within a time of a few hours. At lower concentration, crystallization is much slower and the resulting precipitate has Ba/Ti < 1. Consequently, ceramics sintered from non completely transformed powders will contain a significant amount of the $Ba_6Ti_{17}O_{40}$ phase. Even though a small Ti excess can be beneficial for densification and microstructure development of $BaTiO_3$, a large amount of Ti-rich phase is detrimental for the final properties. As pointed out by Lencka and Riman,[1,3,14] crystalline $BaTiO_3$ is the thermodynamically stable phase for the pH-concentration-temperature conditions adopted in the present study and the yield of reaction should be ⩾99.9%. Consequently the amorphous Ti-rich phase initially obtained should be considered as a metastable phase whose formation is driven by the high supersaturation initially existing in the system. The formation of such a metastable phase decreases the driving force available for formation of $BaTiO_3$ and, at low Ba^{2+} concentration, the crystallization of barium titanate is mainly controlled by kinetic effects. The initial stages of $BaTiO_3$ crystallization were only observed at the lowest concentration, $[Ba^{2+}]_0 = 0.062$ mol l^{-1}. The morphological evolution of the solid phase as well as the kinetic data (Fig. 5) support a nucleation and growth process. The crystallisation of $BaTiO_3$ is related to a transformation of the parent amorphous phase. Spherical particles of 100–200 nm were observed to gradually convert in aggregates of very fine particles (< 10 nm). In general, this kind of disintegration process is usually related to the hydroxylation of the polymeric gel generated in the early stage of reaction. Formation of $BaTiO_3$ crystallites then occurs inside these aggregates, probably because the driving force is locally increased by the presence of particles with lower radius of curvature and the diffusion distance is decreased. The formation of large dendritic-like particles at longer times means that heterogeneous nucleation on existing $BaTiO_3$ surfaces is preferred over homogeneous nucleation. In other words, nucleation is difficult and probably represents the rate-controlling step of the overall process. At intermediate concentration (0.086 mol/1 ⩽ $[Ba^{2+}]$ ϕ ⩽ 0.18 mol/1) the crystallization of $BaTiO_3$ is believed to follow a two-steps mechanism with nucleation and growth of $BaTiO_3$ nanocrystals of ≈60 nm followed by aggregation of these crystallites to form particles up to 300 nm. At high concentration (⩾0.3 mol l^{-1}), the aggregation step is suppressed and the final particles mainly correspond to single nanocrystals of 20–50 nm.

The increase of the unit cell volume of $BaTiO_3$ decreasing the crystallite size has been reported by different authors.[32–35] However, in the present case (see Fig. 2) the unit cell volume is significantly higher than that previously reported for pseudocubic $BaTiO_3$, even for very small particles. For example, Li and Shih [35] reported a cubic cell edge of 4.023 Å for particles of ≈40 nm obtained by hydrothermal treatment at 150 °C, to be compared with values of ≈4.04 Å measured in this work for particles of comparable size. The reference values reported for cubic $BaTiO_3$ at 400–500 K are in the range 3.996–4.012 Å, i.e. lower than those usually measured on fine powders. The peculiar crystallographic properties of the present powders can be related, other than to a size effect, to the presence of a large number of OH^- groups inside the perovskite lattice. This lattice hydroxyl groups produced sharp absorption bands in IR and Raman spectra.[27] According to Waser,[36] the OH^- lattice group corresponds to a proton bonded to an oxygen anion on its regular lattice site. The resulting excess of positive charge must be compensated by the creation of compensating defects, like metal vacancies, electrons or acceptor impurities. Hennings et al.[6,37] have shown that in fine hydrothermal $BaTiO_3$ powders obtained at 150 °C from Ba–Ti acetate gel precursors, the hydroxyl lattice groups are compensated by an equal number of barium and titanium vacancies, i.e. $[OH^{\bullet}] = 6[V''_{Ba}] = 6[V''''_{Ti}]$ according to the notation of Kröger and Vink for lattice defects. Thus, the formula unit of hydroxylated $BaTiO_3$ can be written as $Ba_{(1-x/6)}(V''_{Ba})_{x/6}Ti_{(1-x/6)}(V''''_{Ti})_{x/6}(OH^{\bullet})_xO_{3-x}$. The theoretical density corresponding to one formula unit per unit cell was computed from the measured weight loss in the range 100–800 °C and the XRD unit cell

volume for powders close to stoichiometry ($[Ba^{2+}]_0 \geqslant 0.18$ mol l^{-1}). Comparison with experimental density values shows a good agreement (within $\pm 2\%$). The value of x resulting from calculation is ≈ 0.75. i.e. ≈ 0.86 mol of protons per mole of $BaTiO_3$ are incorporated in the lattice. For compensation with a single type of vacancy (barium or titanium) the calculated densities differ from the experimental value of $\approx 10\%$ and a significant deviation from stoichiometry should be observed. Therefore the defect model proposed for hydrothermal $BaTiO_3$[6,37] also applies to powders synthesized below 100 °C. Interestingly, the weight loss as well as the proton concentration are twice the values reported by Hennings et al.[6] From the analysis of available literature it turns out that a close correlation exists between the temperature of hydrothermal treatment, the amount of water incorporated in the lattice and the pseudocubic cell parameter. For example, the hydrothermal powders obtained by Shi et al.[9] at 300 °C (size 150 nm) showed a weight loss $< 1\%$ related to bulk hydroxyl groups. Accordingly, the cubic lattice parameter was 4.008 Å, very close to that expected for defect-free cubic $BaTiO_3$. Small weight losses were also measured by Asiae et al.[8] for powders obtained at 240 °C. On the contrary, the $BaTiO_3$ powders synthesized by Vivekanandan and Kutty[4] at 90 °C from a TiO_2 gel suspended in a 0.2 M solution of $Ba(OH)_2$ showed a weight loss of $\approx 4.5\%$ and the lattice parameter was very large, 4.065 Å.

5. Summary and conclusions

In this work, experiments of precipitation of barium titanate, $BaTiO_3$, in aqueous solution have been performed. In particular, nanosized (≈ 30 nm) to submicron crystalline particles of $BaTiO_3$ have been obtained by direct reaction between liquid $TiCl_4$ and $Ba(OH)_2$ in aqueous solution at 85 °C and pH $\geqslant 13$. This method represents a simplification in the preparation of $BaTiO_3$ by avoiding the use of a gel or crystalline TiO_2 precursor, as in conventional hydrothermal synthesis. The experimental results support a two-steps reaction mechanism. Initially, a Ti-rich amorphous precipitate is obtained when $TiCl_4$ comes in contact with the aqueous solution. The amorphous phase transforms in crystalline $BaTiO_3$ by reaction with the remaining Ba^{2+} ions left in solution. Whilst the first step is in any case very fast, the crystallisation kinetics is strongly affected by barium concentration and a critical threshold of ≈ 0.12 mol l^{-1} exists. At lower concentrations the final product consists of a mixture of amorphous Ti-rich phase and $BaTiO_3$ even for very long times. Therefore, formation of $BaTiO_3$ with a yield $\geqslant 99.9\%$, even if possible according to thermodynamic calculations for the experimental conditions adopted in the present study, is hindered or strongly slowed down by kinetic factors below the critical barium concentration. Concentration has also a strong influence on crystallite and particle size. The particles obtained for $[Ba^{2+}] \geqslant 0.3$ mol l^{-1} correspond to individual nanosized crystallites (≈ 30 nm). As the barium concentration decreases the size of the crystallites increases to 50–60 nm and the observed particles (100–300 nm) correspond to tight aggregates of the primary crystallites. Powders obtained at high concentration ($[Ba^{2+}] \geqslant 0.18$ mol l^{-1}) contain a large concentration of lattice hydroxyl groups, ≈ 0.85 mol of hydroxyl ions per mole of $BaTiO_3$. The defect model proposed for hydrothermal $BaTiO_3$ also applies to powders obtained in this work.

Acknowledgements

We would like to thank Mr. C. Uliana, Department of Chemistry and Industrial Chemistry, University of Genoa, for TEM observations and Dr. P. Traverso, ICMM-CNR, Genoa for AAS measurements. The staff of the Powder Technology Laboratory, Swiss Federale Institute of Technology, Lausanne, Switzerland is gratefully acknowledged for the technical support.

References

1. Venigalla, S., Advanced materials and powders, barium titanate. *Am. Ceram. Soc. Bull.*, 2001, **6**, 63–64.
2. Hennings, D., Review of chemical preparation routes for barium titanate. *Br Ceram. Proc.*, 1989, **41**, 1–10.
3. Nanni, P., Viviani, M. and Buscaglia, V., Synthesis of dielectric ceramic materials. In *Handbook of Low and High Dielectric Constant Materials and Their Applications*, ed. H. S. Nalwa. Academic Press, San Diego, CA, 1999, pp. 429–455.
4. Vivekanandan, R., Philip, S. and Kutty, T. R. N., Hydrothermal preparation of $Ba(Zr,Ti)O_3$ fine powders. *Mater. Res. Bull.*, 1986, **22**, 99–108.
5. Hennings, D., Rosenstein, G. and Schreinemacher, H., Hydrothermal preparation of barium titanate from barium-titanium acetate gel precursors. *J. Eur. Ceram. Soc.*, 1991, **8**, 107–115.
6. Hennigs, D. and Schreinemacher, S., Characterization of hydrothermal barium titanate. *J. Eur. Ceram. Soc.*, 1992, **9**, 41–46.
7. Kumazawa, H., Annen, S. and Sada, E., Hydrothermal synthesis of barium titanate fine particles from amorphous and crystalline titania. *J. Mater. Sci.*, 1995, **30**, 4740–4744.
8. Asiaie, R., Zhu, W., Akbar, S. A. and Dutta, P. K., Characterization of submicron particles of tetragonal $BaTiO_3$. *Chem. Mater.*, 1996, **8**, 226–234.
9. Shi, E.-W., Xia, C.-T., Zhong, W.-Z., Wang, B.-G. and Feng, C.-D., Crystallographic properties of hydrothermal barium titanate crystallites. *J. Am. Ceram. Soc.*, 1997, **80**, 1567–1572.
10. Pinceloup, P., Courtois, C., Leriche, A. and Thierry, B., Hydrothermal synthesis of nanometer-sized barium titanate powders: control of barium/titanium ratio, sintering, and dielectric properties. *J. Amer. Ceram. Soc.*, 1999, **82**, 3049–3056.
11. Oren, E. E. and Tas, A. C., Hydrothermal synthesis of Dy-doped $BaTiO_3$ powders. *Metall. Mater. Trans.*, 1999, **30B**, 1089–1093.

12. Hu, M. Z.-C., Kurian, V., Payzant, E. A., Rawn, C. J. and Hunt, R. D., Wet-chemical synthesis of monodispersed barium titanate particles—hydrothermal conversion of TiO_2 microspheres to nanocrystalline $BaTiO_3$. *Powd. Tech*., 2000, **110**, 2–14.
13. Lencka, M. M. and Riman, R. E., Thermodynamic modeling of hydrothermal synthesis of ceramic powders. *Chemistry of Materials*, 1993, **5**, 61–70.
14. Lencka, M. M. and Riman, R. E., Hydrothermal synthesis of perovskite materials: thermodynamic modeling and experimental verification. *Ferroelectrics*, 1994, **151**, 159–164.
15. Nanni, P., Leoni, M., Buscaglia, V. and Aliprandi, G., Low-temperature aqueous preparation of barium metatitanate powders. *J. Eur. Ceram. Soc*., 1994, **16**, 85–90.
16. Her, Y.-S., Matijevic, E. and Chon, M. C., Preparation of well-defined colloidal barium titanate crystals by the controlled double-jet precipitation. *J. Mater. Res*., 1995, **10**, 3106–3114.
17. Leoni, M., Viviani, M., Nanni, P. and Buscaglia, V., Low-temperature aqueous synthesis (LTAS) of ceramic powders with perovskite structure. *J. Mater. Sci. Lett*., 1996, **15**, 1302–1304.
18. Her, Y.-S., Lee, S.-H. and Matijevic, E., Continuous precipitation of colloidal particles. II. SiO_2, $Al(OH)_3$ and $BaTiO_3$. *J. Mater. Res*., 1996, **11**, 156–161.
19. Kumar, V., Solution-precipitation of fine powders of barium titanate and strontium titanate. *J. Am. Ceram. Soc*., 1999, **82**, 2580–2584.
20. Grohe, B., Miehe, G. and Wegner, G., Additive controlled crystallization of barium titanate powders and their application for thin-film ceramic production: part I. Powder synthesis. *J. Mater. Res*., 2001, **16**, 1901–1910.
21. Viviani, M., Lemaitre, J., Buscaglia, M. T. and Nanni, P., Low-temperature aqueous synthesis (LTAS) of $BaTiO_3$: a statistical design of experiment approach. *J. Eur. Ceram. Soc*., 2000, **20**, 315–320.
22. Bowen, P., Donnet, M., Testino, A., Viviani, M., Buscaglia, M. T., Buscaglia, V. and Nanni, P., Synthesis of barium titanate powders by low-temperature aqueous synthesis using a new segmented flow tubular reactor. *Key Eng. Mater*., 2002, **206–213**, 21–24.
23. Warren, B. E., *X-Ray Diffraction*. Addison-Wesley, Reading, MA, 1969.
24. O'Bryan Jr., H. M. and Thomson Jr., J., Phase equilibria in the TiO_2-rich region of the system BaO-TiO_2. *J. Am. Ceram. Soc*., 1974, **57**, 522–526.
25. Javadpour, J. and Eror, N. G., Raman spectroscopy of higher titanate phases in the $BaTiO_3$-TiO_2 system. *J. Am. Ceram. Soc*., 1988, **71**, 206–213.
26. Klug, H. P. and Alexander, L. E., *X-Ray Diffraction Procedures*. J. Wiley, New York, 1974.
27. Busca, G., Buscaglia, V., Leoni, M. and Nanni, P., Solid-state and surface spectroscopic characterization of $BaTiO_3$ fine powders. *Chemistry of Materials*, 1994, **6**, 955–961.
28. Vivekanandan, R. and Kutty, T. R. N., Characterization of barium titanate fine powders formed from hydrothermal crystallization. *Powd. Tech*., 1989, **57**, 181–192.
29. Christian, J. W., *The Theory of Transformations in Metals and Alloys*. Pergamon, Oxford, 1981.
30. Hérard, C., Faivre, A. and Lemaître, J., Surface decontamination treatments of undoped $BaTiO_3$—part I: powder and green body properties. *J. Eur. Ceram. Soc*., 1995, **15**, 135–143.
31. Kreuer, K. D., Aspects of the formation and mobility of protonic charge carriers and the stability of perovskite-type oxides. *Solid State Ionics*, 1999, **125**, 285–302.
32. Uchino, K., Sadanaga, E. and Hirose, T., Dependence of the crystal structure on particle size in barium titanate. *J. Am. Ceram. Soc*., 1989, **72**, 1555–1558.
33. Caboche, G. and Niepce, J. C., Dielectric constant of fine grain $BaTiO_3$. *Ceram. Trans*., 1993, **32**, 339–345.
34. Begg, B. D., Vance, E. R. and Nowotny, J., Effect of particle size on the room-temperature crystal structure of barium titanate. *J. Am. Ceram. Soc*., 1994, **77**, 3186–3192.
35. Li, X. and Shih, W.-H., Size effects in barium titanate particles and clusters. *J. Am. Ceram. Soc*., 1997, **80**, 2844–2852.
36. Waser, R., Solubility of hydrogen defects in doped and undoped $BaTiO_3$. *J. Am. Ceram. Soc*., 1988, **71**, 58–63.
37. Hennings, D. F. K., Metzmacher, C. and Schreinemacher, B. S., Defect chemistry and microstructure of hydrothermal barium titanate. *J. Am. Ceram. Soc*., 2001, **84**, 179–182.